Journal of Quantitative Spectroscopy & Radiative Transfer 112 (2011) 2826–2834

Contents lists available at SciVerse ScienceDirect

Journal of Quantitative Spectroscopy & Radiative Transfer

journal homepage: www.elsevier.com/locate/jqsrt

Effect of algae pigmentation on photobioreactor productivity and scale-up: A light transfer perspective

Thomas E. Murphy, Halil Berberoğlu *

Mechanical Engineering Department, Cockrell School of Engineering, The University of Texas at Austin – Austin, TX 78712, USA

ARTICLE INFO

Article history:
Received 5 July 2011
Accepted 28 August 2011
Available online 6 September 2011

Keywords:
Algae
Photobioreactor
Light transport
Photosynthesis
Pigmentation
Scale-up

ABSTRACT

This paper reports a numerical study coupling light transfer with photosynthetic rate models to determine the size and microorganism concentration of photobioreactors based on the pigmentation of algae to achieve maximum productivity. The wild strain *Chlamydomonas reinhardtii* and its transformant *tla1* with 63% lower pigmentation are used as exemplary algae. First, empirical models of the specific photosynthetic rates were obtained from experimental data as a function of local irradiance using inverse methods. Then, these models were coupled with the radiative transfer equation (RTE) to predict both the local and total photosynthetic rates in a planar photobioreactor (PBR). The optical thickness was identified as the proper scaling parameter. The results indicated that under full sunlight corresponding to about 400 W/m^2 photosynthetically active irradiation, enhancement of PBR productivity up to 30% was possible with *tla1*. Moreover, under similar irradiation, optical thicknesses above 169 and 275 for the wild strain and *tla1*, respectively, did not further enhance PBR productivity. Based on these results guidelines are provided for maximizing PBR productivity from a light transport perspective.

1. Introduction

Advanced biofuel production using algal biomass offers a clean and sustainable alternative to fossil fuels [1–3]. However, photosynthetic efficiency of algae cultivation as mass cultures remains a major challenge [4,5]. In particular, light utilization by an algal culture within a photobioreactor (PBR) must be maximized. Wild strains of algae found in the nature have adapted to survive in areas of limited light availability [5]. As a result, their photosystems feature large light harvesting pigment antennae which are responsible for absorbing incident irradiation and transferring that energy to the photosynthetic reaction centers [6]. A negative consequence of this adaptation is that they deliver excessive energy to the reaction centers under larger irradiance that results in photoinhibition, decreasing the cell's photosynthetic rate [7–9]. Furthermore, over-absorption of light by the cells close to the PBR surface deprives the cells in the bulk from sufficient irradiation needed for photosynthesis, known as photolimitation [5].

As a remedy, use of green algae with less pigmentation, formally known as truncated pigment antennae have been proposed for increasing the photosynthetic rate and efficiency of mass cultures in PBRs [4,5,10]. Such organisms could increase the efficiency of mass cultures by (i) shifting photoinhibition to a higher irradiance and (ii) enabling light to penetrate deeper, thus increasing the rate of photosynthesis within the bulk of the PBR [4,5]. Mitra and Melis experimentally demonstrated the proof of concept for increasing the productivity of mass cultures using truncated antenna transformants [5]. However, this was performed only at a single microorganism concentration and the relative contributions of preventing

* Corresponding author. Tel.: +1 512 232 8459; fax: 1 512 471 1045.
E-mail address: berberoglu@mail.utexas.edu (H. Berberoğlu).

0022-4073/$ - see front matter © 2011 Elsevier Ltd. All rights reserved.
doi:10.1016/j.jqsrt.2011.08.012

Nomenclature

C_{chl}	chlorophyll concentration per cell, mol/cell
E_{ext}	mass extinction cross-section, m^2/kg
G	irradiance, W/m^2
I_λ	spectral intensity, $W/m^2/nm/sr$
K_i	inhibition irradiance, W/m^2
K_s	saturation irradiance, W/m^2
k	absorption index
L	thickness of the photobioreactor (PBR), m
N	cell number concentration, $\#/m^3$
P''	total areal production rate, mol/m^2s
X	biomass concentration, kg/m^3
z	distance from light-facing surface of PBR, m

Greek symbols

β	extinction coefficient, m^{-1}
$\overline{\gamma_{O_2}}$	average oxygen production rate per mole of chlorophyll, mol O_2/mol chl/s
δ	Kronecker delta function
κ	absorption coefficient, m^{-1}
λ	wavelength, nm
π_{O_2}	local specific oxygen production rate, mol O_2/cell/s
$\overline{\pi_{O_2}}$	average specific oxygen production rate, mol O_2/cell/s
σ	scattering coefficient, m^{-1}
θ_c	angle of incidence of collimated light, rad

Subscripts

abs	absorption
c	collimated light
d	diffuse light
eff	effective radiation characteristics
inc	incident
m	medium
max	maximum
O_2	oxygen
PAR	photosynthetically active radiation

photoinhibition and deeper light penetration for increasing the PBR productivity were not evaluated. Moreover, because such experiments require significant time and resources to perform, it is of interest to estimate the performance of a photobioreactor using a numerical tool. Such a tool would also enable analysis and optimization of photobioreactor design as well as the derivation of guidelines for microorganism engineering. Thus, this study aims to (i) model the photosynthetic productivity of algae as a function of their pigmentation and local photosynthetically active irradiance, (ii) couple these models with accurate light transfer models to assess the local and total productivity of high cell density cultures with different pigment content, and (iii) define scaling parameters to guide the design and scale up of outdoor photobioreactors for maximum productivity. As exemplary organisms, the wild and *tla1* strains of the green algae *Chlamydomonas reinhardtii* were utilized in this study as experimental data on both the productivity and radiation characteristics were available in the literature [5,11].

2. Current state of knowledge

2.1. Cell pigmentation and light transfer in a photobioreactor

Photosynthetic cells can naturally vary their pigmentation in response to nutrient concentrations as well as to available irradiance [12]. As an algae culture reaches larger cell density in mass cultivation, the cells tend to get over pigmented due to limited light penetration [13]. However, it is possible to permanently limit the cell pigmentation by genetic engineering [10].

Polle et al. have engineered *C. reinhardtii*, a unicellular green algae species, to have a total of 0.9×10^{-15} moles of chlorophyll per cell as opposed to 2.4×10^{-15} moles in its wild strain [5,10]. They called this engineered strain truncated light harvesting antenna 1 (*tla1*). Berberoglu et al. reported the experimentally measured radiation characteristics of both the wild and the genetically engineered strain in the spectral region of photosynthetically active radiation [11]. The results showed that the absorption cross-section of *tla1* was about 34% smaller than that of the wild strain over this spectrum. However, the reduction in the absorption cross-section was compensated by an increase in the scattering cross-section and the overall extinction coefficient was not significantly affected. Considering that the scattering albedo of these systems is greater than 0.5, scattering is a significant phenomenon in light transport in PBRs and careful radiation transfer analysis is needed to assess the benefits of low cell pigmentation for enhancing light penetration and PBR productivity [11,14].

2.2. Photosynthetic activity and modeling

During photosynthesis, photosynthetically active radiation (PAR), defined from 400 to 700 nm, is absorbed by the light harvesting antennae made of pigment molecules such as chlorophyll a, b and carotenoids [6]. In oxygenic photosynthesis, such as in algae and higher plants, this energy is transferred to the photosystems and is utilized to oxidize a mole of water to generate two moles of electrons, two moles of protons and half a mole of molecular oxygen [6]. The protons and electrons are used to generate energy and electron carriers, namely, ATP and NADPH, that are used in Calvin cycle to convert carbon dioxide to sugars [6]. The rate of CO_2 fixation can be considered as the photosynthetic rate and the stoichiometry is such that per mole of CO_2 fixed, one mole of O_2 is generated [15]. Thus, it is possible to track the rate of photosynthesis with the oxygen evolution rate [16,17].

At the same time, the light energy that is transferred to the photosystems also causes photodamage [9,18]. Under low irradiation, the rate of repair of the photosystem is as fast as the rate of photodamage and the reaction center operates at near maximum efficiency. However, under larger irradiance, the rate of photodamage exceeds the rate of repair, which results in photoinhibition [6–8]. Photoinhibition can be permanent or temporary, but it decreases the rate of photosynthesis. Moreover, it has been proposed that the irradiance at which photoinhibition becomes significant is inversely proportional to the chlorophyll content of the cells [5]. Thus, truncating the pigment antennae of algae can increase the efficiency of mass cultures via two distinct mechanisms [5,10,11]. First, truncated-antenna algae can potentially have a higher critical irradiance for photoinhibition than wild strain cells because less excitation energy is delivered to the reaction centers [5]. Second, decreasing the cellular chlorophyll content decreases the cell's absorption cross-section, which enables deeper light penetration into the culture. It is of interest to determine the relative significance of these processes in order to achieve photosynthetically efficient photobioreactors.

Several models have been used to predict the specific photosynthetic rate or the specific growth rate of various algal strains as functions of irradiance [19–23]. Although photoinhibition is a well-documented phenomenon, not all models reported previously account for it [19–21]. In studies by Molina Grima et al. and by Aiba, photoinhibition was accounted for by the use of the Aiba equation [22,23]. These studies were used to assess the productivity of photobioreactors without taking into account the scattering phenomena by the microorganisms. On the other hand, Cornet and Dussap constructed a PBR productivity model that couples the radiative transport equation, which takes microorganism scattering into account, with a growth kinetic model [24]. However, their model also neglected photoinhibition. This paper contributes to the effort of understanding the local productivity to improve the total productivity of photobioreactors through a numerical study, from light transport and light utilization perspective, taking into account light absorption and scattering, photoinhibition, and pigmentation of algae cells.

3. Analysis

Consider a plane-parallel photobioreactor (PBR) of thickness L equal to 1 cm as shown in Fig. 1. It contains algae at a biomass concentration of X kg/m^3 and is irradiated with normally incident collimated light of intensity $I_{c,\lambda,in}$ as well as diffuse light of intensity $I_{d,\lambda,in}$ at the surface of the reactor. As light penetrates into the PBR, it is absorbed by the liquid phase and the microorganisms and scattered anisotropically by the microorganisms.

3.1. Assumptions

In order to make the problem mathematically tractable it is assumed that: (1) light transfer is one-dimensional as the system is symmetric in the plane of the photobioreactor, (2) the reactor is well mixed and microorganisms are uniformly distributed and randomly oriented in the reactor, (3) the liquid phase is non-emitting, cold, weakly absorbing, and non-scattering in the photosynthetically active region (PAR) of the solar spectrum, (4) both surfaces of the photobioreactor are treated with an anti-reflective coating and are perfectly transmitting in the spectral range of interest. It is further assumed that (5) the microorganisms are cultivated with no nutrient limitations, and (6) the reactor is kept isothermal at 25 °C with the aid of an active temperature control, and thus (7) the specific oxygen production rate π_{O_2}, i.e., the rate of photosynthesis, depends only on the local irradiance available to the microorganisms. Note also that for algae cells 10 μm in diameter in a suspension at biomass concentrations up to 2 kg/m^3 (corresponding to 1.5 $\times 10^{13}$ cells/m^3), independent scattering dominates over dependent scattering [11].

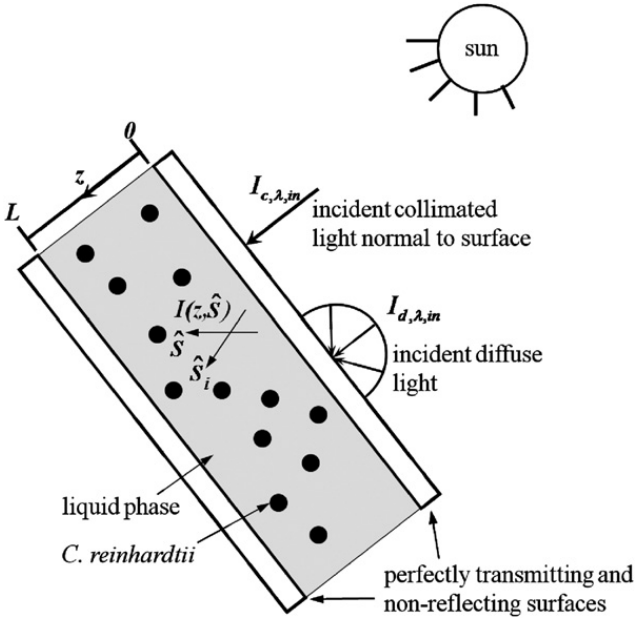

Fig. 1. Schematic of photobioreactor system.

3.2. Governing equations and boundary conditions

The transport of light within a photobioreactor is governed by the radiative transport equation (RTE), and the total intensity $I_\lambda(z,\hat{s})$ at a given location z in direction $\hat{s}$ can be given as the sum of the collimated $I_{c,\lambda}(z,\hat{s})$ and the diffuse components $I_{d,\lambda}(z,\hat{s})$ [14,24,25]. The steady-state RTE for the collimated intensity can be written as [26]

$$\frac{\partial I_{c,\lambda}(z,\hat{s})}{\partial z} = -\beta_{eff,\lambda} I_{c,\lambda}(z,\hat{s}) \tag{1}$$

where $\beta_{eff,\lambda}$ is the effective extinction coefficient expressed as

$$\beta_{eff,\lambda} = \kappa_{eff,\lambda} + \sigma_{eff,\lambda} \tag{2}$$

where $\kappa_{eff,\lambda}$ and $\sigma_{eff,\lambda}$ are the effective spectral absorption and scattering coefficients of the microorganism suspension in PBR, respectively [14].

Moreover, the steady-state RTE for the diffuse intensity can be written as [26]

$$\frac{\partial I_{d,\lambda}(z,\hat{s})}{\partial z} = -\beta_{eff,\lambda} I_{d,\lambda}(z,\hat{s}) + \frac{\sigma_{eff,\lambda}}{4\pi}\int_{4\pi} I_{d,\lambda}(z,\hat{s}_i)\Phi_\lambda(\hat{s}_i,\hat{s})\, d\Omega_i + \frac{\sigma_{eff,\lambda}}{4\pi}\int_{4\pi} I_{c,\lambda}(z,\hat{s}_i)\Phi_\lambda(\hat{s}_i,\hat{s})\, d\Omega_i \quad (3)$$

where Φ_λ is the scattering phase function of the microorganisms which represents the probability that radiation traveling in the solid angle $d\Omega_i$ around the direction $\hat{s}_i$ will be scattered into the solid angle $d\Omega$ around direction $\hat{s}$. The first integral term in Eq. (3) accounts for the in-scattered diffuse radiation whereas the second one corresponds to the in-scattered collimated radiation from an arbitrary direction $\hat{s}_i$ into the direction of interest $\hat{s}$.

The boundary conditions for the collimated intensity on each end of the PBR can be given as

$$I_{c,\lambda}(0,\theta) = G_{c,\lambda,in}\delta(\theta-\theta_c) \quad \text{for } 0 \le \theta \le \pi$$

$$I_{c,\lambda}(L,\theta) = 0 \quad \text{for } \pi \le \theta \le 2\pi \quad (4)$$

where $\delta(\theta-\theta_c)$ is the Kronecker delta function and $G_{c,\lambda,in}$ is the spectral collimated solar irradiation incident on the PBR surface at an angle of θ_c as reported by Gueymard et al. [27]. The angle of incidence θ_c in this case is zero for normally incident radiation. At the same time, the diffuse component of the intensity at each end can be given as

$$I_{d,\lambda}(0,\theta) = G_{d,\lambda,in}/\pi \quad \text{for } 0 \le \theta \le \pi$$

$$I_{d,\lambda}(L,\theta) = 0 \quad \text{for } \pi \le \theta \le 2\pi \quad (5)$$

where $G_{d,\lambda,in}$ is the diffuse solar irradiation incident on the PBR and reported by Gueymard et al. [27].

3.3. Radiation characteristics of the medium and microorganisms

The radiation characteristics of the liquid medium were assumed to be those of pure water in the spectral range from 400 to 700 nm. The spectral absorption coefficient of the medium is given by [28]

$$\kappa_{m,\lambda} = \frac{4\pi k_\lambda}{\lambda} \quad (6)$$

where k_λ is the absorption index of water [29].

Moreover, the radiation characteristics of *C. reinhardtii* wild strain and *tla1* in the spectral range from 350 to 710 nm, as well as their asymmetry parameter, g, for the Henyey–Greenstein scattering phase function approximation, were experimentally measured and reported by Berberoglu et al. [11].

3.4. Photosynthetic rate modeling

Due to its simplicity and capacity to describe photoinhibition, the Aiba function was used in this study to model local specific oxygen production as [23]

$$\pi_{O_2}(z) = \pi_{O_2,max}\frac{G_{PAR}(z)}{K_s + G_{PAR}(z) + \frac{1}{K_i}G_{PAR}(z)^2} \quad (7)$$

where $\pi_{O_2,max}$ is the maximum specific production rate in mol O_2/cell/s, G_{PAR} is the local irradiance in the PAR in W/m^2, and K_s and K_i are the saturation and inhibition irradiances, respectively, expressed in W/m^2. Finally, the total oxygen production rate for the PBR per unit surface area is then calculated as

$$P''_{O_2} = \int_0^L \pi_{O_2}(z) N\, dz \quad (8)$$

where N is the number density of the cells in cells/m^3, assumed to be uniform and independent of location z.

Mitra and Melis have recently reported the O_2 production rates of both wild and *tla1* cultures of *C. reinhardtii* as a function of incident irradiance [5]. In order to recover the Aiba model parameters from the experimental data (i) first the local irradiance within the PBR was simulated using the RTE and (ii) an inverse method employing a least squares method was used to estimate the coefficients $\pi_{O_2,max}$, K_s, and K_i that matched the total O_2 production rate reported by Mitra and Melis. For these simulations, the irradiance spectrum of the fluorescent lamps employed in the study (Ecologic by Sylvania, USA and Fluorex by Lights of America, USA) which was reported with a spectral resolution of 10 nm was used [30]. Fig. 2 shows the solution procedure for the inverse method. Note that Mitra and Melis reported the oxygen production rate in their experiments per mole of chlorophyll instead of per cell [5]. Thus, the results can be related to each other using the chlorophyll content per cell namely, 2.4×10^{-15} mol chl/cell for wild strain and 0.9×10^{-15} mol chl/cell for *tla1* [5].

3.5. Solution procedure

The RTE was solved using the discrete ordinates method employing a Gaussian quadrature having 24 directions per hemisphere along with weight factors successfully used for strongly forward scattering media [14]. The local spectral intensity was integrated using the Gaussian quadrature to obtain the local spectral irradiance which was then integrated over the spectral range

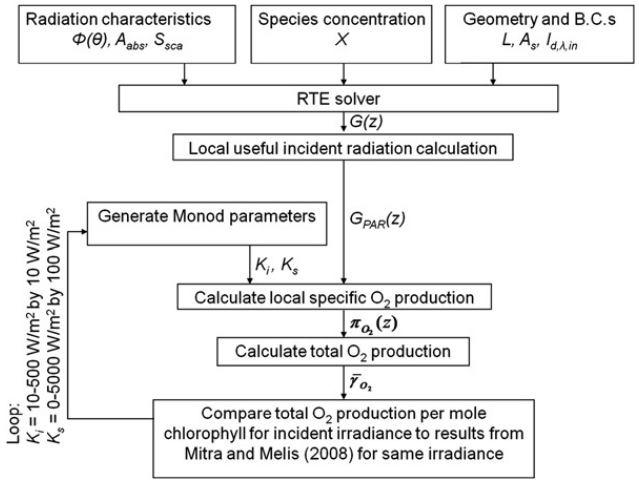

Fig. 2. Flow chart of the inverse method for recovering the Aiba model parameters from experimental data.

from 400 to 700 nm using the trapezoidal integration method. Finally, the local specific O_2 production rate was calculated and integrated using the trapezoidal integration method to obtain the total photosynthetic rate of the PBR. A grid sensitivity study was performed to ensure that the local specific O_2 production rate $\pi_{O_2}(z)$ was independent of grid size. At 1200 points along the z-direction, doubling the number of points did not change $\pi_{O_2}(z)$ by more than 1% and thus was used in the study.

4. Results and discussion

4.1. Specific oxygen production rate for each strain

Fig. 3 compares the average oxygen production rates obtained in this study using the Aiba model to those reported experimentally in Ref. [5]. It shows that the model predicts the experimental oxygen production rates with an average error of 3% for the wild strain and 1% for *tla1*. Table 1 summarizes the model parameters obtained for the wild strain and for *tla1*. It shows that both the saturation irradiance, K_s, and the inhibition irradiance, K_i, are larger for *tla1* than for the wild strain by 33% and 50%, respectively. This indicates that the critical irradiance at which photoinhibition becomes significant for *tla1* is larger than that for the wild strain.

Fig. 4 shows the cellular oxygen production rate as a function of local irradiance in the PAR for both strains. It indicates that the wild strain had a higher oxygen production rate than *tla1* at local irradiances less than 170 W/m^2 in the PAR, whereas *tla1* had a greater oxygen production rate at irradiances greater than 170 W/m^2. Moreover, it shows that the maximum local oxygen production rate, $\pi_{O_2}(z)$, for the wild strain was 120×10^{-18} mol O_2/cell/s at the local irradiance of 67 W/m^2. At this irradiance, the specific oxygen production rate for the wild strain is 16% greater than that for *tla1*. Finally, it shows that the maximum oxygen production rate for *tla1* was 108×10^{-18} mol O_2/cell/s at the local irradiance of 97 W/m^2.

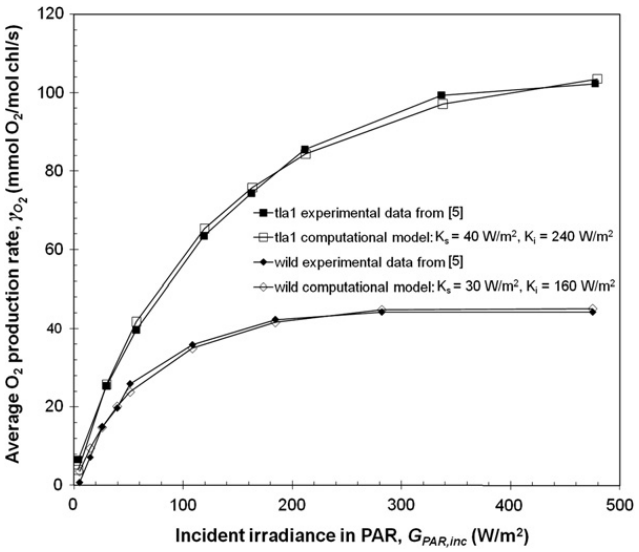

Fig. 3. Comparison of numerical and experimental results for average oxygen production rate per mole of chlorophyll as a function of incident irradiation in the PAR.

Table 1
Aiba model parameters for wild and *tla1* strains of *C. reinhardtii*.

Strain	$\pi_{O_2,max}$ (mol O_2 cell^{-1} s^{-1})	K_s (W/m^2)	K_i (W/m^2)
Wild	225×10^{-18}	30	160
tla1	196×10^{-18}	40	240

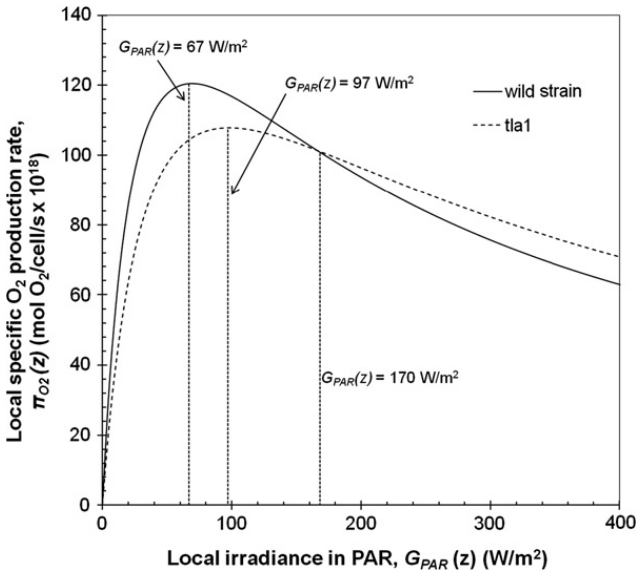

Fig. 4. Aiba models for the local specific O_2 production rate of the wild strain and *tla1* as a function of local irradiance in PAR. For the wild strain, K_s = 30 W/m^2, K_i = 160 W/m^2. For *tla1*, K_s = 40 W/m^2, K_i = 240 W/m^2.

These results can be interpreted in terms of the size of the pigment antennae for each strain. At a given irradiance, the large pigment antennae of the wild strain provide the photosystems with more energy than do the smaller pigment antennae of *tla1*. Large pigment antennae are thus advantageous at low irradiance, when photosynthesis is light-limited, but disadvantageous at high irradiance, when photosynthesis is light-inhibited as the excessive energy delivered to the photosystems causes photoinhibition.

4.2. Optical thickness and light transport in the PBR

The photosynthetic efficiency of a photobioreactor is a strong function of the local irradiance in the photosynthetically active region (PAR) available for the cells. Local irradiance is a function of the distance from the light-facing side of the photobioreactor as well as the absorption and scattering cross-sections of the algae. Thus, the non-dimensional parameter the local optical thickness $\tau(z)$ can be used to take these variables into account simultaneously. It can be defined for the PBR over the spectral range of PAR as [31]

$$\tau(z)_{PAR} = \overline{\beta}_{eff,PAR} z \tag{9}$$

where z is the physical distance from the light-facing surface and $\overline{\beta}_{eff,PAR}$ is the average effective extinction coefficient weighted by the spectrum of the incident intensity in the PAR given as [31]

$$\overline{\beta}_{eff,PAR} = \frac{\int_{400}^{700} \beta_{eff,\lambda} I_{tot,\lambda,in} d\lambda}{\int_{400}^{700} I_{tot,\lambda,in} d\lambda} \tag{10}$$

Since the spectral absorption coefficient of water $\kappa_{m,\lambda}$ is on the order of 0.1 m^{-1} in the PAR and the mass extinction cross-section of the microorganisms is on the order of 1000 m^2/kg in the PAR, for microorganism concentrations used in this study (X greater than 0.1 kg/m^3), the absorption by the medium can be neglected with an error on $\beta_{eff,\lambda}$ of less than 1%. Thus, the local optical thickness can be expressed as a linear function of microorganism concentration as

$$\tau(z) \cong \overline{E}_{ext,PAR} X z \tag{11}$$

where $\overline{E}_{ext,PAR}$ is the weighted average of the mass extinction cross-section over the PAR, equal to 857 m^2/kg and 917 m^2/kg for the wild strain and *tla1*, respectively. Fig. 5 shows the local oxygen production rate as a function of local optical thickness for PBRs containing the wild strain at three different microorganism concentrations. The figure demonstrates that the oxygen production rate is a function of the optical thickness, regardless of the particular combination of the physical thickness and microorganism concentration.

Moreover, Berberoglu et al. showed that although the absorption cross-section of less pigmented cells was 34% smaller than that of the fully pigmented cells, their scattering cross-section was larger by about 16% [11]. Thus, the enhancement of light penetration in a PBR using the less pigmented cells requires careful radiation transfer analysis, properly taking into account the scattering phenomena. Fig. 6 shows the local irradiance in the PAR

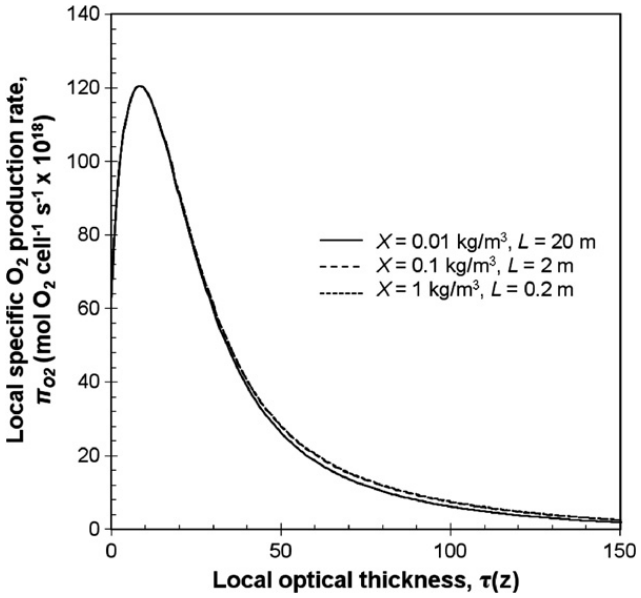

Fig. 5. Local oxygen production rate as a function of local optical thickness for three combinations of PBR physical thickness and microorganism concentration for the wild strain. The PBR optical thickness τ_{PBR} is 171 for all three cases.

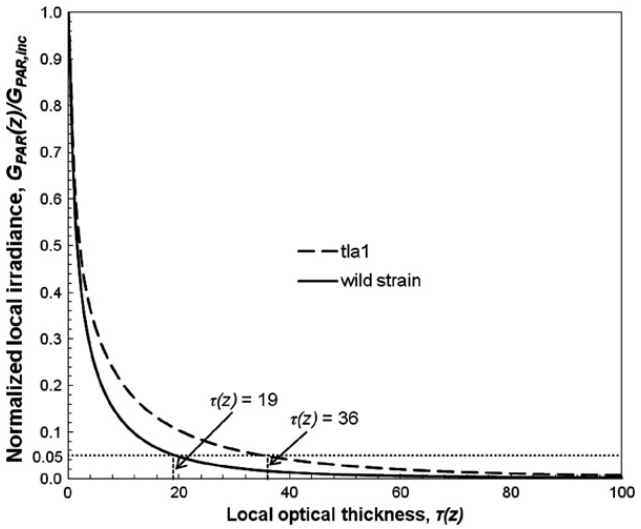

Fig. 6. Local irradiance in the PAR normalized by the incident irradiance as a function of local optical thickness for the wild strain and *tla1*.

normalized by the incident irradiance as a function of local optical thickness for both the wild strain and *tla1*. It indicates that for a given microorganism concentration and PBR thickness, the local irradiance is larger for *tla1*. In particular, the incident irradiation is attenuated by 95% at an optical thickness of 19 for the wild strain whereas this level of attenuation was attained for *tla1* at an optical thickness of 36. Using the results of RTE, the local photosynthetic rates of the microorganisms can be determined according to the Aiba model to assess the enhancement of the PBR productivity employing less pigmented cells.

4.3. Effect of incident irradiance, optical thickness and cell pigmentation on PBR productivity

Fig. 7(a) and (b) shows the local specific oxygen production rates as a function of local optical thickness under incident solar irradiances of 400 W/m^2 and 40 W/m^2 in the PAR, respectively. In order to demonstrate the effect of incident irradiance, a high irradiance of 400 W/m^2 in the PAR roughly corresponding to full sunlight conditions and one tenth of this, 40 W/m^2, as the low irradiance were used in this analysis. For both cases, the maximum local specific oxygen production rate was largest for the wild strain. However, at local optical thicknesses greater than 15 and 8 for 400 W/m^2 and 40 W/m^2 incident irradiances, respectively, the oxygen production rate of *tla1* culture exceeded that of the wild strain culture. In addition, Fig. 7(c) and (d) shows the total oxygen production rates per unit surface area of PBR P''_{O_2} as a function of the total optical thickness of the PBR τ_{PBR} under incident solar irradiances of 400 W/m^2 and 40 W/m^2 in the PAR, respectively. It illustrates that at smaller optical thicknesses, the PBR containing the wild strain had larger productivity than one containing *tla1*. For 400 W/m^2 and 40 W/m^2 incident irradiance, the use of *tla1* culture displayed larger productivity at optical thicknesses greater than 37 and 42, respectively. This also indicates that the maximum benefit of using less pigmented cells such as *tla1* can be realized at large incident irradiances and large optical thicknesses, i.e., large cell concentrations and/or

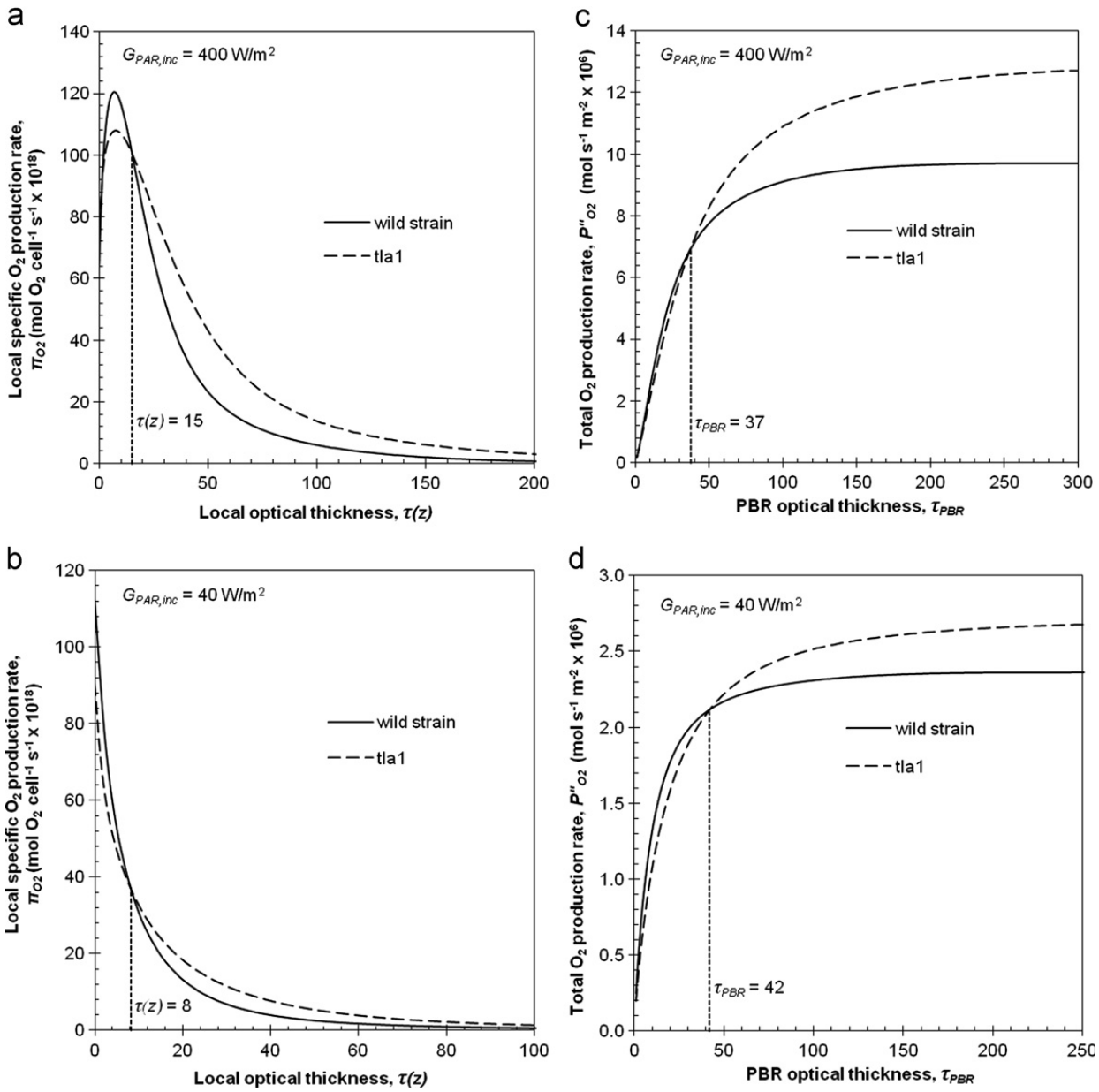

Fig. 7. Local specific oxygen production rate as a function of local optical thickness for wild strain and *tla1* under an incident irradiance in the PAR of (a) 400 W/m^2 and (b) 40 W/m^2. Also, the total oxygen production rate per unit PBR surface area for wild strain and *tla1* under an incident irradiance in the PAR of (c) 400 W/m^2 and (d) 40 W/m^2. The cell biomass concentration was 1 kg/m^3 for all cases.

thick PBRs in the direction of light propagation. However, this cross-over point was shown to have a weak dependence on incident irradiance.

Furthermore, Fig. 7 indicates that beyond a certain optical thickness the local productivity becomes negligible and further increase in optical thickness, either by increasing microorganism concentration or the physical thickness of the PBR, does not significantly improve productivity. Thus, a cutoff value, nominated as dead zone optical thickness τ_{dz}, is defined beyond which the total O_2 production rate increases by less than 1% of its maximum value. Fig. 8 shows the dead zone optical thickness τ_{dz} as a function of incident irradiance in the PAR for the wild strain and *tla1*. It indicates that τ_{dz} is always larger for *tla1* than for the wild strain and it increases with increasing incident irradiance. Thus, τ_{dz} is a function of both the incident irradiance in the PAR and the mass absorption cross-section $A_{abs,i}$ of the organisms. From a practical perspective, it is desirable to model τ_{dz} to guide the design of PBRs, i.e., the thickness and microorganism concentration, based on cell pigmentation and available solar radiation at a particular geographical location for maximizing productivity. A simple model for τ_{dz} for both microorganisms can be given as

$$\tau_{dz}(G_{PAR,inc},A_{abs,i}) = \frac{A_{abs,wild}}{A_{abs,i}}(C_1 G_{PAR,inc}^3 + C_2 G_{PAR,inc}^2 + C_3 G_{PAR,inc} + C_4) \quad (12)$$

where the coefficients C_1 through C_4 are 1.947×10^{-6} $[W/m^2]^{-3}$, -1.972×10^{-3} $[W/m^2]^{-2}$, 0.796 $[W/m^2]^{-1}$, and 42.08 were obtained using the least squares fitting

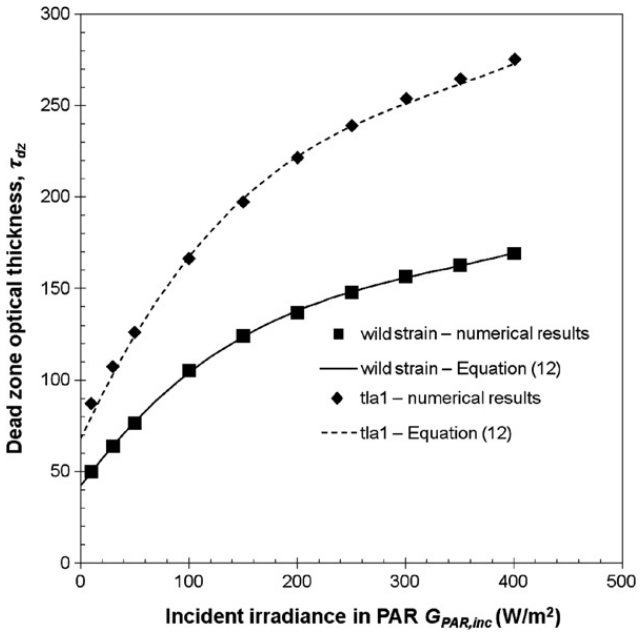

Fig. 8. Local optical thickness corresponding to the onset of dead zone for wild strain and *tla1* as a function of incident irradiance in the PAR.

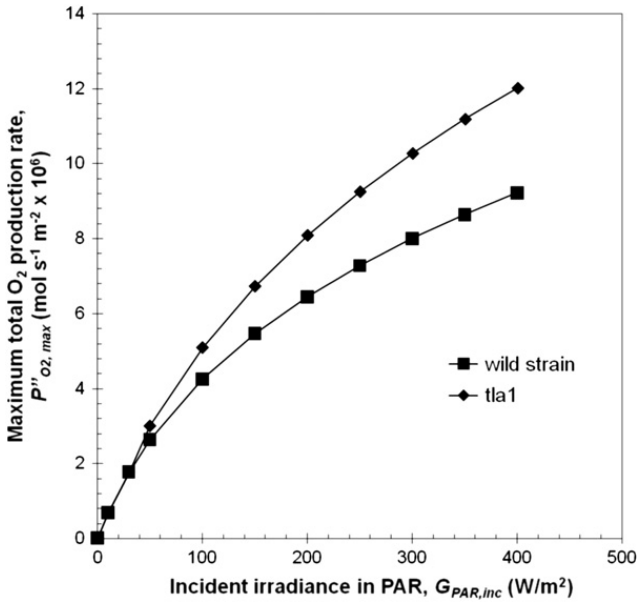

Fig. 9. Maximum total oxygen production rate per unit PBR surface area for wild strain and *tla1* as a function of incident irradiance in the PAR. The cell biomass concentration was 1 kg/m^3 for all cases.

method [32]. This function is recommended over the range of incident solar irradiances from 10 to 400 W/m^2 in the PAR. Over this range, the average error for the critical optical thickness between the numerical results and Eq. (12) is 0.6% and 1.8% for the wild strain and *tla1*, respectively.

Finally, Fig. 9 shows the maximum oxygen production rate $P''_{O_2,max}$ as a function of incident solar irradiance in the PAR for PBRs having an optical thickness equal to the dead zone optical thickness at that particular incident irradiance. The figure indicates that at irradiances less than 50 W/m^2, there is no appreciable difference between the productivities of *tla1* and the wild strain. In this low irradiance regime, the wild strain's poor light transmittance in mass culture is balanced by its larger specific cellular oxygen production rate. However, at larger incident irradiances, the productivity of *tla1* culture increases at a faster rate than that of the wild strain, resulting in about 30% larger oxygen production rate at 400 W/m^2.

5. Conclusions

This numerical study assessed the effect of using genetically engineered algae strains with reduced pigment concentration on the light transfer and photosynthetic rate of photobioreactors. To achieve this, first, the specific oxygen production rate as a function of local irradiance was obtained from experimental data for *C. reinhardtii* wild strain and its truncated chlorophyll antenna transformant *tla1*. Then, the specific oxygen production rates were coupled with the radiative transfer equation (RTE) to determine the local and total photosynthetic rates in a plane-parallel photobioreactor under solar irradiance. Based on the results obtained, the following conclusions can be drawn:

- The maximum recommended photobioreactor optical thickness, defined based on their respective extinction coefficients, is 169 and 275 for *C. reinhardtii* wild strain and *tla1*. For optical thicknesses beyond these values, there is not enough light for the algae to undergo appreciable photosynthesis.
- Use of *tla1* has negligible effect on increasing productivity for irradiances less than 50 W/m^2 in the PAR. However, at larger irradiances, improvements of up to 30% were possible with *tla1*.
- The dominant mechanism for the greater productivity of *tla1* in mass culture is *tla1*'s decreased mass absorption cross-section, which enables light to penetrate deeper within the PBR. The maximum specific oxygen production rate per cell is greater for the wild strain than it is for *tla1*. Therefore, truncation of pigment antennae through genetic engineering must seek a balance between the enhanced light penetration and the decreased maximum specific oxygen production rate of truncated-antenna cultures.

Finally, the tools presented and the results in this study are expected to aid designers to optimize photobioreactor depth and the corresponding microorganism concentration as a function of cell pigmentation from a light transport perspective for maximum photosynthetic productivity.

References

[1] Demirbas A. Use of algae as biofuel sources. Energy Conversion and Management 2010;51(12):2738–49.
[2] Beer LL, Boyd ES, Peters JW, Posewitz MC. Engineering algae for biohydrogen and biofuel production. Current Opinion in Biotechnology 2009;20(3):264–71.
[3] Subhadra B, Edwards M. An integrated renewable energy park approach for algal biofuel production in United States. Energy Policy 2010;38(9):4897–902.

[4] Melis A. Solar energy conversion efficiencies in photosynthesis: minimizing the chlorophyll antennae to maximize efficiency. Plant Science 2009;177(4):272–80.
[5] Mitra M, Melis A. Optical properties of microalgae for enhanced biofuels production. Optics Express 2008;16(26):21807–20.
[6] Blankenship RE. In: Molecular mechanisms of photosynthesis. Oxford: Blackwell Science Ltd.; 2002.
[7] Murata N, Takahashi S, Nishiyama Y, Allakhverdiev SI. Photoinhibition of photosystem II under environmental stress. Biochimica et Biophysica Acta, Bioenergetics 2007;1767(6):414–21.
[8] Sharma PK, Singhal GS. Influence of photoinhibition on photosynthesis and lipid peroxidation. Journal of Photochemistry and Photobiology, B 1992;13(1):83–94.
[9] Hakala M, Tuominen I, Keränen M, Tyystjärvi T, Tyystjärvi E. Evidence for the role of the oxygen-evolving manganese complex in photoinhibition of photosystem II. Biochimica et Biophysica Acta, Bioenergetics 2005;1706(1–2):68–80.
[10] Polle JEW, Kanakagiri S, Melis A. *tla1* a DNA insertional transformant of the antenna size. Planta 2003;217:49–59.
[11] Berberoglu H, Pilon L, Melis A. Radiation characteristics of *Chlamydomonas reinhardtii* CC125 and its truncated chlorophyll antenna transformants *tla1*, *tlaX* and *tla1-CW+*. International Journal of Hydrogen Energy 2008;33(22):6467–83.
[12] Masuda T, Tanaka A, Melis A. Chlorophyll antenna size adjustments by irradiance in *Dunaliella salina* involve coordinate regulation of chlorophyll a oxygenase (CAO) and Lhcb gene expression. Plant Molecular Biology 2003;51(5):757–71.
[13] Nakajima Y, Ueda R. Improvement of photosynthesis in dense microalgal suspension by reduction of light harvesting pigments. Journal of Applied Phycology 1997;9(6):503–10.
[14] Berberoglu H, Yin J, Pilon L. Light transfer in bubble sparged photobioreactors for H_2 production and CO_2 mitigation. International Journal of Hydrogen Energy 2007;32(13):2273–85.
[15] Mohammad P. In: Handbook of photosynthesis. Hoboken, NJ, USA: CRC Press; 2005.
[16] Brindley C, Acien FG, Fernandez-Sevilla JM. The oxygen evolution methodology affects photosynthetic rate measurements of microalgae in well-defined light regimes. Biotechnology and Bioengineering 2010;106(2):228–37.
[17] Jeon Y, Cho C, Yun Y. Measurement of microalgal photosynthetic activity depending on light intensity and quality. Biochemical Engineering Journal 2005;27(2):127–31.
[18] Murata N, Takahashi S, Nishiyama Y, Allakhverdiev S. Photoinhibition of photosystem II under environmental stress. Biochimica et Biophysica Acta 2007;1767(6):414–21.
[19] Molina Grima E, Garca Camacho F, Sanchez Perez JA, Fernandez Sevilla J, Acien Fernandez FG, Contreras Gomez A. A mathematical model of microalgal growth in light limited chemostat cultures. Journal of Chemical Technology & Biotechnology 1994;61:167–73.
[20] Bannister TT. Quantitative description of steady state, nutrient-saturated algal growth, including adaptation. Limnology and Oceanography 1979;24(1):76–96.
[21] Tessier G. Croissance des populations bactériennes et quantité d'aliment disponible. Revue Scientifique Paris 1942;80:209.
[22] Molina Grima E, Garca Camacho F, Acien Fernandez FG, Chisti Y. Photobioreactors: light regime, mass transfer, and scaleup. Journal of Biotechnology 1999;70(1–3):231–47.
[23] Aiba S. Growth kinetics of photosynthetic microorganisms. Advances in Biochemical Engineering 1982;23:85–156.
[24] Cornet J-F, Dussap C-G. A simple and reliable formula for assessment of maximum volumetric productivities in photobioreactors. Biotechnology Progress 2009;25(2):424–35.
[25] Siegel R, Howell J. In: Thermal radiation heat transfer. 4th ed. New York: Taylor & Francis; 2002.
[26] Modest MF. In: Radiative heat transfer. San Diego, CA: Academic Press; 2003.
[27] Gueymard CA, Myers D, Emery K. Proposed reference irradiance spectra for solar energy system testing. Solar Energy 2002;73(6):443–67.
[28] Bohren CF, Huffman DR. In: Absorption and scattering of light by small particles. New York: John Wiley & Sons; 1998.
[29] Hale GM, Querry MR. Optical constants of water in the 200-nm to 2000-nm wavelength region. Applied Optics 1973;12(3):555–63.
[30] Berberoğlu H, Barra N, Pilon L, Jay JA. Growth, CO_2 consumption, and H_2 production of *Anabaena variabilis* ATCC 29413-U under different irradiances and CO_2 concentrations. Journal of Applied Microbiology 2008;104:105–21.
[31] Berberoglu H, Pilon L. Maximizing the solar to H_2 energy conversion efficiency of outdoor photobioreactors using mixed cultures. International Journal of Hydrogen Energy 2010;35(2):500–10.
[32] Riley KF. In: Essential mathematical methods for the physical sciences. Leiden: Cambridge University Press; 2010.